Geomechanical constitutive modelling of a chalk partly saturated by oil and water

By F. Collin[1], P. Delage[2], C. Schroeder[3] and R. Charlier[1]
[1]Département MSM, Université de Liège, Belgique
[2]CERMES, Ecole Nationale des Ponts et Chaussées, France
[3]Département LGIH, Université de Liège, Belgique

and ALERT Geomaterials

Paper proposed to the EUROCK 2000 Symposium, 27-31 March 2000, Aachen
13/08/08

ABSTRACT: Chalk in oil reservoir is generally saturated by two or more different fluids. In this paper, a constitutive law is proposed for the modelling of the mechanical behaviour of a chalk. The effects of the capillary pressure are taken into account. They are considered as an independent variable, as in the Barcelona's basic model developed for unsaturated clay. On the other hand, internal friction and pore collapse are modelled as independent mechanisms. Eventually, the model predictions are compared with experimental results.

1. Introduction

This paper deals with chalk oil reservoirs, as found for instance in the North Sea oilfields. Due to geological history (4), chalk pores are partly saturated by oil and water (and sometimes by gas also). Chalk deposited in marine environment was initially saturated by seawater. Then oil migrated, and progressively intruded the pores, remaining some residual water menisci at intergranular contacts.

Capillary pressures develop, thanks to interface tensions between oil and water. Evidence of capillary pressure effects in geomechanics has been first investigated in fine-grained soils (see 5 for example). More recently, tests were performed on chalk samples saturated by oil and water (4). In soil mechanics, different authors (5, 6) developed constitutive models where the air-water suction is taken as an independent variable, and where suction modifies the shape of the yield surface. The chalk constitutive models proposed by (7) and (3) take the oil-water suction into account, and can predict deformations linked to suction changes during water injection. The aim of this paper is to develop a constitutive model for a chalk partly saturated by oil and water, based on the model proposed by the Barcelona's team (5).

Most experiments carried out on chalks, and most constitutive laws developed consider two plastic mechanisms: the pore collapse and the frictional rupture. Most models consider that the two mechanisms are independent (1), and define two yield surfaces. But special care has to be taken at the intersection between the two yield surfaces, which is an apex that involves some numerical difficulties.

For this reason, models using only one yield surface have also been developed (2, 3). The expression of the surface is more complex, but with no apex. However, difficulties can appear with the definition of hardening rules, because the two basic physical mechanisms are necessarily coupled.

Another solution for apex problems is to use an additional surface to join the two principal yield surfaces, in order to ensure a continuous slope. The apex is avoided, with a total independence between the two mechanisms.

In the paper, the results of some experiments performed on oil and water saturated chalk sample are eventually compared with numerical predictions.

2. Constitutive law

In order to model the two plastic mechanisms; two yield surfaces are combined within a cap model: the modified CamClay model, for pore collapse, and the internal friction model, which concerns the rupture by internal friction.

Another particularity of chalk behaviour is that the traction resistance defined by an internal friction model may be overestimated. A third yield surface is adopted to limit traction stresses.

The yield curve is no more continuously derivable at the intersection of the different curves, leading to numerical difficulties. However, recent publications provided an elegant way to solve this problem (8).

In the model presented here, suction is considered as an independent variable, and suction effects are accounted for using the Barcelona approach (5).

2.1 CAMCLAY MODEL

In the modified CamClay model used, the elastic behaviour can be either linear or non-linear.

In the $(I_\sigma, II_{\hat{\sigma}})$ plane, the CamClay yield surface is elliptic (Fig. 2.1):

$$II_{\hat{\sigma}}^2 + m^2\left(I_\sigma - \frac{3c}{\tan\phi_C}\right)(I_\sigma + 3p_0) = 0 \quad (2.1)$$

where c is the cohesion, ϕ_C is the friction angle in compression path, and p_0 is the preconsolidation pressure, which define the size of the yield surface.

I_σ, $II_{\hat{\sigma}}$, $III_{\hat{\sigma}}$ and β represent respectively the first stress tensor invariant, the second deviatoric stress tensor invariant, the third deviatoric stress tensor invariant, and Lode's angle:

$$I_\sigma = \sigma_{ii} \quad (2.2)$$

$$II_{\hat{\sigma}} = \sqrt{\frac{1}{2}\hat{\sigma}_{ij}\hat{\sigma}_{ij}} \quad (2.3)$$

$$\hat{\sigma}_{ij} = \sigma_{ij} - \frac{I_\sigma}{3}\delta_{ij} \quad (2.4)$$

$$\beta = -\frac{1}{3}sin^{-1}\left(\frac{3\sqrt{3}}{2}\frac{III_{\hat{\sigma}}}{II_{\hat{\sigma}}^{\;3}}\right) \quad (2.5)$$

With $$III_{\hat{\sigma}} = \frac{1}{3}\hat{\sigma}_{ij}\hat{\sigma}_{jk}\hat{\sigma}_{ki} \quad (2.6)$$

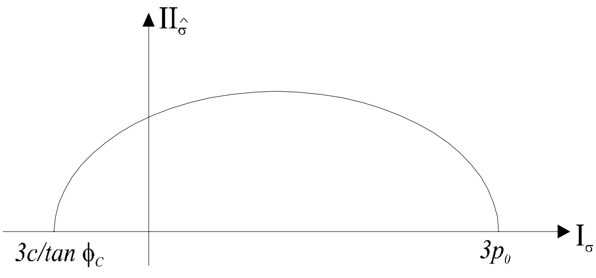

Figure 2.1: CamClay model -$(I_\sigma, II_{\hat{\sigma}})$ plane

A dependence on the third invariant stress is introduced in the model using the parameter m. Therefore, the shape of the surface in the deviatoric plane is not a circle. The coefficient m is defined by:

$$m = a(1 + b\,sin3\beta)^n \quad (2.7)$$

$sin3\beta$ is derived from equation of the third invariant:

$$sin3\beta = -\left(\frac{3\sqrt{3}}{2}\frac{III_{\hat{\sigma}}}{II_{\hat{\sigma}}^3}\right) \quad (2.8)$$

and the three parameters a, b and n must verify different conditions (9).

In a first step, an associated plasticity has been chosen. The flow surface, which defines the direction of plastic deformations and the yield surface are identical.

2.2 INTERNAL FRICTION MODEL

A more sophisticated model can be built from the Drucker-Prager's cone by introducing a dependence on the Lode's angle β, in order to match more closely the Mohr-Coulomb criterion. It consists of a smoothing of the Mohr-Coulomb plasticity surface. The formulation proposed by (9,10) is adopted. It can be written in a very similar way to the Drucker-Prager's criterion:

$$f = II_{\hat{\sigma}} + m\left(I_\sigma - \frac{3c}{\tan\phi_C}\right) = 0 \quad (2.9)$$

where the coefficient m is still defined by equation (2.7). Non-associated plasticity is considered here, and a dilatancy angle ψ, which can change with hardening, has to be defined.

2.3 TRACTION MODEL

Traction stresses allowed by an internal friction model depend on both friction angle and cohesion. Experimental evidences show that this model overestimates the traction stresses in chalk. To avoid this drawback, a third yield surface is introduced by limiting the mean stress in traction, independently of the stress deviator.

In the plane $(I_\sigma, II_{\hat{\sigma}})$, the following relation gives the yield surface:

$$f = I_\sigma - 3\sigma_t = 0 \quad (2.10)$$

Associated plasticity is used for this surface, and no hardening is included.

2.4 LAW INTEGRATION

Because of the three yield surfaces, the integration of the law is complex. One has to determine which plastic mechanism is active, and one has to manage the case where two surfaces are active. This case occurs at the junction of two surfaces: the apex regime is a combination of two mechanisms.

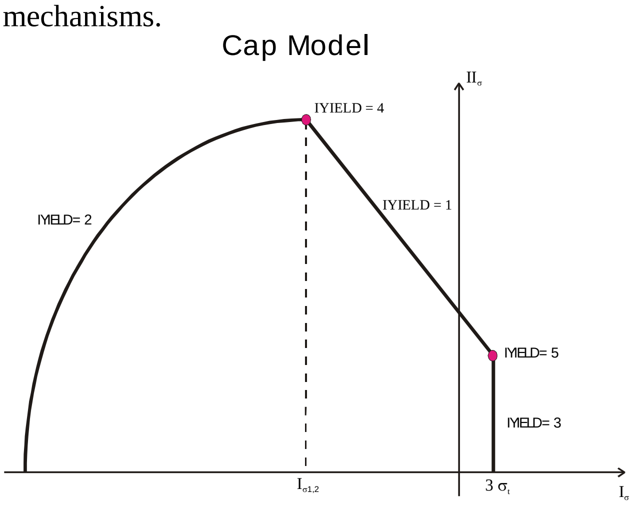

Figure 2.2: Cap Model, combination of three yield surfaces.

Different plastic regimes are possible:

- Internal friction model active: IYIELD = 1
- CamClay model active: IYIELD = 2
- Traction limitation model active: IYIELD = 3
- Combination of Internal friction and CamClay model: IYIELD = 4
- Combination of Internal friction and Traction limitation model: IYIELD = 5.

Integration over time of the general rate constitutive elastoplastic relation leads to the incremental form (10):

$$\Delta\sigma_{ij} = \left(C^{e}_{ijkl} - C^{p}_{ijkl}\right)\Delta\varepsilon_{kl} \qquad (2.11)$$

The method used here is classically based on the operator-split (11), which consists in computing an elastic predictor/plastic corrector. After computing the elastic predictor, the first problem is to determine if either the apex regime or one single surface is active. This question is important only if the stress state is close to an apex. But the notion of proximity is relative and arbitrary. In this model, the following routine has been chosen (See fig. 2.2):

1. Computation of the mean stress at the junction of the internal friction model and CamClay model:

$$I_{\sigma,1-2} = \left(\frac{3c}{tg\phi} - 3p_0\right)/2 \qquad (2.12)$$

2. If $I_\sigma < I_{\sigma,1-2} + \frac{I_{\sigma,1-2}}{2}$, only the CamClay model could be active (YIELD = 2).
3. If $I_{\sigma,1-2} + \frac{I_{\sigma,1-2}}{2} < I_\sigma < I_{\sigma,1-2} - \frac{I_{\sigma,1-2}}{2}$, a combination of the CamClay model and internal friction model could be active (IYIELD = 4).
4. If $I_{\sigma,1-2} - \frac{I_{\sigma,1-2}}{2} < I_\sigma < 3\sigma_t$, only the internal friction model could be active (IYIELD = 1).
5. If $I_\sigma > 3\sigma_t$, a combination of internal friction model and the traction limitation model could be active (IYIELD = 5).

Hughes & Simo (8) proposed a technique of integrating the law in an apex regime. Let's consider a combination of the two plastic mechanisms 1 and 2. The following consistency conditions must be verified:

$$\begin{cases} f_1 = 0 \text{ and } f_2 = 0 \\ \dot{f}_1 = 0 \text{ and } \dot{f}_2 = 0 \end{cases} \qquad (2.13)$$

f_1 and f_2 being the yield surfaces related to the plastic mechanism 1 and 2 respectively.

The total plastic strains is the sum of the plastic strains of the two mechanisms:

$$\dot{\varepsilon}^{p} = \dot{\varepsilon}^{p,1} + \dot{\varepsilon}^{p,2} = \dot{\lambda}^{1}\frac{\partial g_1}{\partial\sigma} + \dot{\lambda}^{2}\frac{\partial g_2}{\partial\sigma} \qquad (2.14)$$

where g_1 and g_2 are respectively the plastic potentials associated to the plastic mechanism 1 and 2. Considering that yield surfaces (f_m, m = 1 to 2) are only function of the stress state (σ_{ij}) and hardening variables (ζ^m), the consistency conditions can be obtained using a Taylor's development:

$$f_m\left(\sigma^{\theta}_{ij} + \Delta\sigma^{p}_{ij}, \varsigma^{m,\theta} + \Delta\varsigma^{m}\right) = f_m\left(\sigma^{\theta}_{ij}, \varsigma^{m,\theta}\right) + \frac{\partial f_m}{\partial\sigma^{\theta}_{ij}}\Delta\sigma^{p}_{ij} + \frac{\partial f_m}{\partial\varsigma^{m,\theta}}\Delta\varsigma^{m} \qquad (2.15)$$

with
$$\Delta\sigma^{p}_{ij} = -C^{e}_{ijkl}\Delta\left(\varepsilon^{p,1}_{kl} + \varepsilon^{p,2}_{kl}\right) \qquad (2.16)$$

$$\Delta\varsigma^{m} = \frac{d\varsigma^{m}}{d\varepsilon^{p,m}} Val^{m}\,\Delta\lambda^{m} \qquad (2.17)$$

Using equations (2.14), (2.16) and (2.17), equation (2.15) can be re-written

$$f_m = f_m\left(\sigma_{ij}^{\theta}, \varsigma^{m,\theta}\right) - \frac{\partial f_m}{\partial \sigma_{ij}^{\theta}} C_{ijkl}^{e} \left(\sum_{n=1}^{2} \Delta\lambda^n \frac{\partial g_n}{\partial \sigma_{kl}^{\theta}} \right) + Val^m \frac{\partial f_m}{\partial \varsigma^{m,\theta}} \frac{d\varsigma^m}{d\varepsilon^{p,m}} \Delta\lambda^m \quad (2.18)$$

Knowing that in the plastic regime f = 0, the previous relation gives a consistency equation for each mechanisms. The system of equations provides the value of the two plastic multiplicators. The value of the plastic multiplicators $\Delta\lambda^1$ and $\Delta\lambda^2$ is obtained by considering that the plastic mechanisms were active.

However, this hypothesis is only verified if the two multiplicators are positive. If one multiplicators is negative, the corresponding mechanism must not be activated, and the computation is reiterated only with the other yield surface.

2.5 SUCTION EFFECT

As mentioned above, the oil-water suction has an effect on the mechanical behaviour of chalk containing oil and water. Suction changes can induce both elastic and plastic strains.

The yield surface in the $\left(I_\sigma, II_{\hat{\sigma}}\right)$ plane is influenced by suction. In order to model all typical behaviour features of unsaturated soils, new yield surfaces, defined in the plane $\left(I_\sigma, II_{\hat{\sigma}}, s\right)$ are necessary (5, 13).

2.5.1 General formulation

The general elastoplastic relations are formulated in their rate form. The strain rate is composed of a mechanical part and of a suction part. Each contribution is partitioned in an elastic and a plastic component:

$$\begin{aligned} \dot{\varepsilon}_{ij} &= \dot{\varepsilon}_{ij}^{m} + \dot{\varepsilon}_{ij}^{s} \\ &= \dot{\varepsilon}_{ij}^{m,e} + \dot{\varepsilon}_{ij}^{s,e} + \dot{\varepsilon}_{ij}^{m,p} + \dot{\varepsilon}_{ij}^{s,p} \end{aligned} \quad (2.19)$$

The mechanical elastic part is linked to the stress tensor following Hooke's law:

$$\tilde{\sigma}_{ij} = C_{ijkl}^{e} \dot{\varepsilon}_{kl}^{m,e} \quad (2.20)$$

where the compliance elastic tensor is defined by

$$C_{ijkl}^{e} = \frac{E}{1+\nu}\delta_{ik}\delta_{jl} + \frac{E\nu}{(1+\nu)(1-2\nu)}\delta_{ij}\delta_{kl} \quad (2.21)$$

And where $\tilde{\sigma}$ is the Jaumann objective stress rate.

The suction elastic part of the strain rate is linked to suction by the following relation:

$$\dot{\varepsilon}_{kl}^{s,e} = \frac{\kappa_s}{(1+e)} \frac{\dot{s}}{(s+p_{at})} \delta_{kl} = h_{kl}^{e} \dot{s} \quad (2.22)$$

Here, a more general framework of non-associated plasticity is considered in order to limit dilatancy, and the plastic flow rate is perpendicular to a plastic potential g (an associated law can be obtained by substituting g by f)

$$\dot{\varepsilon}_{ij}^{m,p} = \dot{\lambda} \frac{\partial g}{\partial \sigma_{ij}} \quad (2.23)$$

The suction plastic part is linked to suction with the following relation:

$$\dot{\varepsilon}_{kl}^{s,p} = \frac{\lambda_s}{(1+e)} \frac{\dot{s}}{(s+p_{at})} \delta_{kl} = h_{kl}^{p} \dot{s} \quad (2.24)$$

Equation (2.19) can be rewritten as:

$$\begin{aligned} \dot{\varepsilon}_{ij} &= \dot{\varepsilon}_{ij}^{m,e} + \dot{\varepsilon}_{ij}^{s,e} + \dot{\varepsilon}_{ij}^{m,p} + \dot{\varepsilon}_{ij}^{s,p} \\ &= C_{ijkl}^{e\,-1} \tilde{\sigma}_{kl} + h_{ij}^{e} \dot{s} + \dot{\lambda} \frac{\partial g}{\partial \sigma_{ij}} + h_{ij}^{p} \dot{s} \end{aligned} \quad (2.25)$$

Considering a general hardening/softening plastic law depending on the internal variable ζ, the consistency condition can be formulated as:

$$\dot{f} = \frac{\partial f}{\partial \sigma_{ij}} \tilde{\sigma}_{ij} + \frac{\partial f}{\partial \zeta} \dot{\zeta} + \frac{\partial f}{\partial s} \dot{s} = 0 \quad (2.26)$$

2.5.2 Yield surfaces

Suction has some effects on the properties of soil. Up to now, we consider that:

- The preconsolidation pressure p_0 changes with suction according to the LC concept of the Barcelona model, giving:

$$p_0 = p_c \left(\frac{p_0^*}{p_c} \right)^{\frac{\lambda(0)-\kappa}{\lambda(s)-\kappa}} \quad (2.27)$$

with $\lambda(s) = \lambda(0)\left[(1-r)\exp(-\beta s) + r\right]$ (2.28)

where p_0^* is the preconsolidation pressure for s = 0, p_c is a reference pressure, κ and λ the elastic and the plastic slope respectively in the oedometric plane.

- Cohesion increases with suction according to the relation:

$$c(s) = c(0) + k\,s \quad (2.29)$$

- The friction angle is not affected by suction.
- Suction is supposed to have no influence on traction resistance σ_t.

The suction dependency of the three yield surfaces is as follows:
- CamClay model:

$$II_{\hat{\sigma}}^2 + m^2\left(I_\sigma - \frac{3c(s)}{\tan\phi_C}\right)\left(I_\sigma + 3p_0(s)\right) = 0 \quad (2.30)$$

- Internal friction model:

$$f = II_{\hat{\sigma}} + m\left(I_\sigma - \frac{3c(s)}{\tan\phi_C}\right) = 0 \quad (2.31)$$

- Traction model: $f = I_\sigma - 3\sigma_t = 0$ (2.32)

With these surfaces, no irreversible strains are induced by a suction increase. A fourth yield criterion, called SI curve, is needed:

$$s - s_0 = 0 \quad (2.33)$$

3. Experimental results and model predictions

Two kinds of experiments on chalk samples have been performed by LGIH and by CERMES along various stress and suction paths: suction controlled oedometer tests, and triaxial tests with chalk samples saturated either by water either by a specific oil called Soltrol 170.

3.1 TRIAXIAL TEST

Experimental results showed that linear elasticity was relevant. The elastic parameters have been determined in the plane (ε_v , p) and (ε_d , q). The elastic part of the path is linear in these planes, and the slope is respectively K and $3G$.

	Water	Soltroll
E (MPa)	1366	1483
ν	0.20	0.18

Table 3.1: Elastic parameters

The yield points correspond to the marked change in slope observed in the plane (ε_v, p). The parameters of the yield surface are defined on the table below.

	Water	Soltroll
ϕ (°)	25	25
c (MPa)	1.5	2.0
p_0 (MPa)	12	18
ψ (°)	25	25

Table 3.2: Strength parameters

Figure 3.1 shows that a good qualitative agreement is obtained between numerical results and experimental data obtained on samples saturated with water or Soltrol.

3.2 OEDOMETER TESTS

Oedometer tests were performed under different controlled suction. Parameters are derived from experimental data.

In the Barcelona model, the κ coefficient is not suction dependent. However, the experimental data reported in Figure 3.2 shows some dependency.

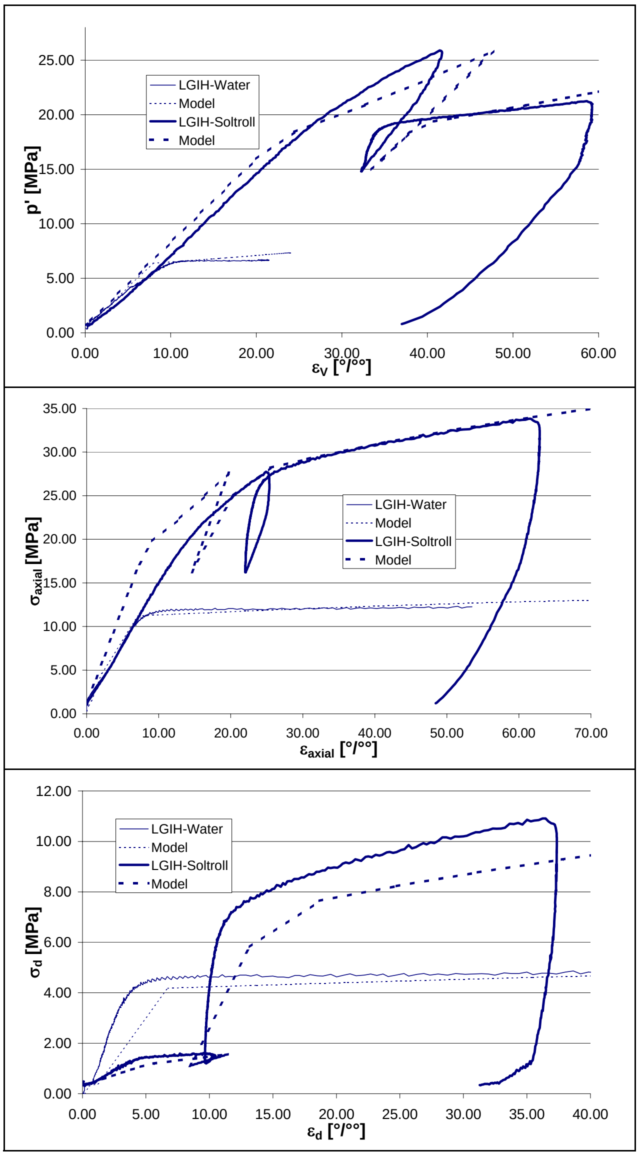

Figure 3.1: Triaxial test on chalk samples.

In the Barcelona model, the compressibility index λ is suction dependent, according to relation (2.28), which is adopted here. This relation has a deep influence on the shape of the LC curve (2.27). The function λ(s) and the reference pressure p_c have been chosen in a manner that the LC curve fits well with the experimental results.

A good qualitative agreement is observed in figure 3.2 between experiment and numerical results.

$\lambda(0)$	r	β (1/MPa)	p_c (MPa)	κ	ν	$p_0(0)$ (MPa)
0.11	0.8	2.00	1.65	0.0085	0.4	7.05

Table 3.3: Parameters

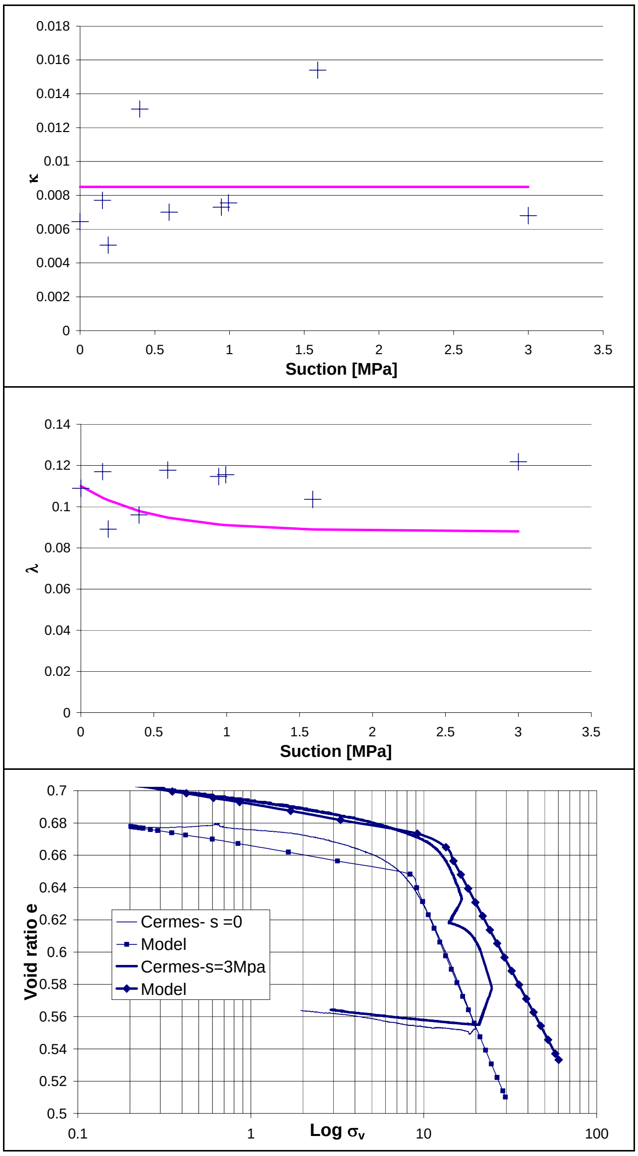

Figure 3.2: Suction controlled oedometer tests.

4. Conclusions

A constitutive law has been developed in order to account for the oil-water capillary effects in reservoir chalks. The model is able to satisfactory reproduce some available experimental data. However, many questions are still opened.

The definition of the parameters κ and λ is not easy. The Barcelona's basic model consider that κ remains constant with suction changes, and that λ changes with suction. Experimental results show that κ changes with suction, whereas λ does not vary much. Some adaptations of the Barcelona model are necessary, and are presently under development. Other aspects, like wettability and creep, are not yet accounted for at present state. They will be considered in the future.

5. Acknowledgments

The authors are grateful to the EC – Joule programme, the FNRS, and the Communauté Française de Belgique for the support received.

References

1. Shao, J.F. & Henry, J.P., 1991. Development of an elastoplastic model for porous rock. *International Journal of plasticity*, Vol. 7, p 1-13.

2. Papamichos, E. Brignoli, M. & Santarelli, F. J., 1997. An experimental and theoretical study of partially saturated collapsible rock. *Mechanics of cohesive-frictional materials*, Vol. 2, pp.251-278.

3. Brignoli, M. Santarelli, F. J. & Righetti, C., 1994. Capillary phenomena in an impure chalk. *Eurock'94*.

4. Delage, P. Schroeder, Ch. & Cui,Y.J, 1996. Subsidence and capillary effects in chalk. *Eurock 96 Proc.*, Turin, pp. 1291 – 1298.

5. Alonso, E. E. Gens, A. & Josa, A., 1990. A constitutive model for partially saturated soils. *Géotechnique* 40 (3), pp 405-430.

6. Bolzon, G. & Schrefler, B. A., October 1995. State surfaces of partially saturated soils: an effective pressure approach, *Apl. Mech. Rev.* 48 (10), American Society of Mechanical Engineers.

7. Maury, V. Piau, J-M & Halle, G., Oct. 1996. Subsidence induced by water injection in water sensitive reservoir rocks : the example of Ekofisk. *5th North Sea Chalk Symposium, Reims.*

8. Simo, J.C. & Hughes, T.J.R., 1998. Computational Inelasticity. *Interdisciplinary applied mathematics* (7): pp. 198-218.

9. Van Eekelen, H.A.M., 1980. Isotropic yield surfaces in three dimensions for use in soil mechanics. *International Journal for Numerical and Analytical Methods in Geomechanics* (4), pp. 98-101.

10. Barnichon, J-D., 1998. Finite Element Modelling in Structural and Petroleum Geology. *Thèse de doctorat*, MSM – Université de Liège.

12.Simo, J.C. & Taylor, R.L., 1985. Consistent tangent operators for rate-independent elastoplasticity. *Computer Method in Applied Mechanics and Engineering* 48, pp. 101-118.

13. Li, XL., 1999. Comportement hydromécanique des sols fins : de l'état saturé à l'état non saturé. *Thèse de doctorat*, MSM – Université de Liège.